

Re–Os and U–Pb geochronological constraints on the eclogite–tonalite connection in the Archean Man Shield, West Africa

Matthias G. Barth^{a,*}, Roberta L. Rudnick^{a,1}, Richard W. Carlson^b,
Ingo Horn^{a,2}, William F. McDonough^{a,3}

^a Department of Earth and Planetary Sciences, Harvard University, 20 Oxford Street, Cambridge, MA 02138, USA

^b Department of Terrestrial Magnetism, Carnegie Institution of Washington, 5241 Broad Branch Road NW, Washington, DC 20015, USA

Received 12 December 2001; accepted 27 August 2002

Abstract

Mantle-derived eclogite xenoliths and tonalite–trondhjemite–granodiorites (TTG) that occur in the Man Shield, West Africa, sample different levels of Archean lithosphere. Chemical and oxygen isotope systematics indicate that low MgO eclogites from the Koidu kimberlite are ancient remnants of subducted oceanic crust that may have been involved in regional Archean crust formation. Re–Os whole rock isotopic data for these eclogites scatter about a line with slope corresponding to an Archean age of 3.44 ± 0.76 Ga (2σ), with Re–Os model ages ranging from 1.4 to 3.9 Ga. This wide range of model ages overlaps with the age range for crust formation and metamorphism in the Man Shield. In situ U–Pb ages of zircons from crustal rocks have been measured by laser ablation ICP-MS. A tonalitic gneiss has discordant zircons with rare old cores (~ 3.6 Ga) and an upper concordia intercept at 2890 ± 9 Ma (2σ). Zircons from a mafic lower crustal granulite xenolith are concordant at 2686 ± 32 Ma. Our results, together with previously published ages for Man Shield rocks, indicate an early Archean crust formation event followed by major crustal growth at 2.9–3.0 Ga and a last major metamorphic event at 2.7 Ga. These data show that the eclogites and the continental crust of the West African Craton overlap in time of formation (but only at the very broad age uncertainty provided by the eclogite Re–Os results). They are permissive of Archean crustal growth by melting of the protoliths of the materials now sampled as the Koidu eclogite xenoliths. If so, this suggests that Archean crustal growth in the Man Shield occurred in a convergent margin setting.

© 2002 Elsevier Science B.V. All rights reserved.

Keywords: Eclogite; Tonalite–trondhjemite–granodiorite; Archean crustal growth; West African Craton

* Corresponding author. Present address: Department of Petrology, Faculty of Earth Sciences, Utrecht University, Budapestlaan 4, 3584 CD Utrecht, The Netherlands. Tel.: +31-30-253-5071; fax: +31-30-253-5030

E-mail address: barth@post.harvard.edu (M.G. Barth).

¹ Present address: Department of Geology, University of Maryland, College Park, MD 20742, USA.

² Present address: Institut für Mineralogie, Universität Hannover, Callinstrasse 3, 30167 Hannover, Germany.

³ Present address: Department of Geology, University of Maryland, College Park, MD 20742, USA.

1. Introduction

Tonalite–trondhjemite–granodiorites (TTG) composition and gray gneisses, their high-grade metamorphic equivalent, are a major constituent of the Earth's early continental crust (Martin, 1994, and references therein). Based on their major element compositions and strongly fractionated rare earth element (REE) patterns, these rocks appear to be derived from a mafic, garnet-bearing (i.e. deep seated) source, such as subducted oceanic crust or mafic parts of the lowermost continental crust. Mantle-derived eclogite xenoliths carried in kimberlites have been interpreted as former oceanic crust and may represent residues generated during TTG production (Helmstaedt and Doig, 1975; MacGregor and Manton, 1986; Taylor and Neal, 1989; Ireland et al., 1994; Jacob et al., 1994; Schulze et al., 1997). This hypothesis has been proposed based on circumstantial evidence of general complementary geochemical characteristics in the two groups of rocks (Ireland et al., 1994; Rollinson, 1997). Better constraints on the age and origin of eclogite xenoliths are thus important for understanding Archean crustal growth processes.

Both mantle-derived eclogite xenoliths and Archean TTG occur in the Man Shield, West Africa. The eclogites from the Mesozoic Koidu kimberlite complex, Sierra Leone, fall into two groups, based on distinct major element and mineral chemistry (Hills and Haggerty, 1989; Fung and Haggerty, 1995): a high MgO group (> 16 wt.% MgO in the whole rock) and a low MgO group (6–13 wt.% MgO). Major and trace element systematics indicate that the low MgO eclogites have residual compositions complementary to granitoids from the Man Shield, suggesting that both were derived from a common basaltic parent rock with a composition similar to greenstone belt basalts in Sierra Leone (Rollinson, 1997; Barth et al., 2001). Variable oxygen isotope ratios of the low MgO eclogites are consistent with an origin as remnants of subducted oceanic crust (Barth et al., 2001). The high MgO eclogites from Koidu, while carried in the same kimberlite pipe, have distinctive petrographic, chemical, and petrologic features from the low MgO group. The high MgO eclogites also exhibit systematically higher equilibration tem-

peratures than the low MgO eclogites. Thus, there is no indication that they share a common origin. Trace element modeling suggests a low-P origin as plagioclase–pyroxene–olivine cumulates for some high MgO eclogites and a higher-P origin as garnet–pyroxene cumulates in the uppermost mantle ($P < 3$ GPa) for others (Barth et al., 2002).

The objective here is to provide age constraints for portions of a vertical section of the Archean Man Shield of Sierra Leone, using the U–Pb and Re–Os methods. The Re–Os isotope system potentially provides a means of high-precision ages for mafic rocks such as eclogite xenoliths from the Koidu kimberlite. This is because Re behaves as an incompatible element during mantle melting, whereas Os is highly compatible and remains in the source (e.g. Allègre and Luck, 1980). Consequently, eclogitic xenoliths, a lithology which traditionally have been difficult to date, have high Re/Os ratios, and will develop very radiogenic Os isotopic compositions over time (Pearson et al., 1995b; Menzies et al., 1998). Furthermore, the Re–Os isotope system appears less sensitive to the metasomatism that severely affects incompatible-element-based isotope systems in eclogitic xenoliths (e.g. Snyder et al., 1993).

2. Geological setting and previous geochronological work

The West African Craton consists of two major basement domains of Archean and Paleoproterozoic age, the Reguibat Rise in the north and the Leo Rise in the south (Fig. 1). They are separated by the Proterozoic to Paleozoic sedimentary basin of Taoudéni and are entirely surrounded by Panafrican and Hercynian belts. The Proterozoic parts of these two domains have been well studied and apparently arose from a major crustal growth event at approximately 2.1 Ga (e.g. Abouchami et al., 1990; Boher et al., 1992). In contrast, Archean terrains from the West African Craton have not been extensively studied. Recent geochronological studies of the Amsaga area, in the southwestern Reguibat Rise, confirm the Archean age of this area and demonstrate the presence of Early Archean relicts (ca. 3.5 Ga) in the basement of

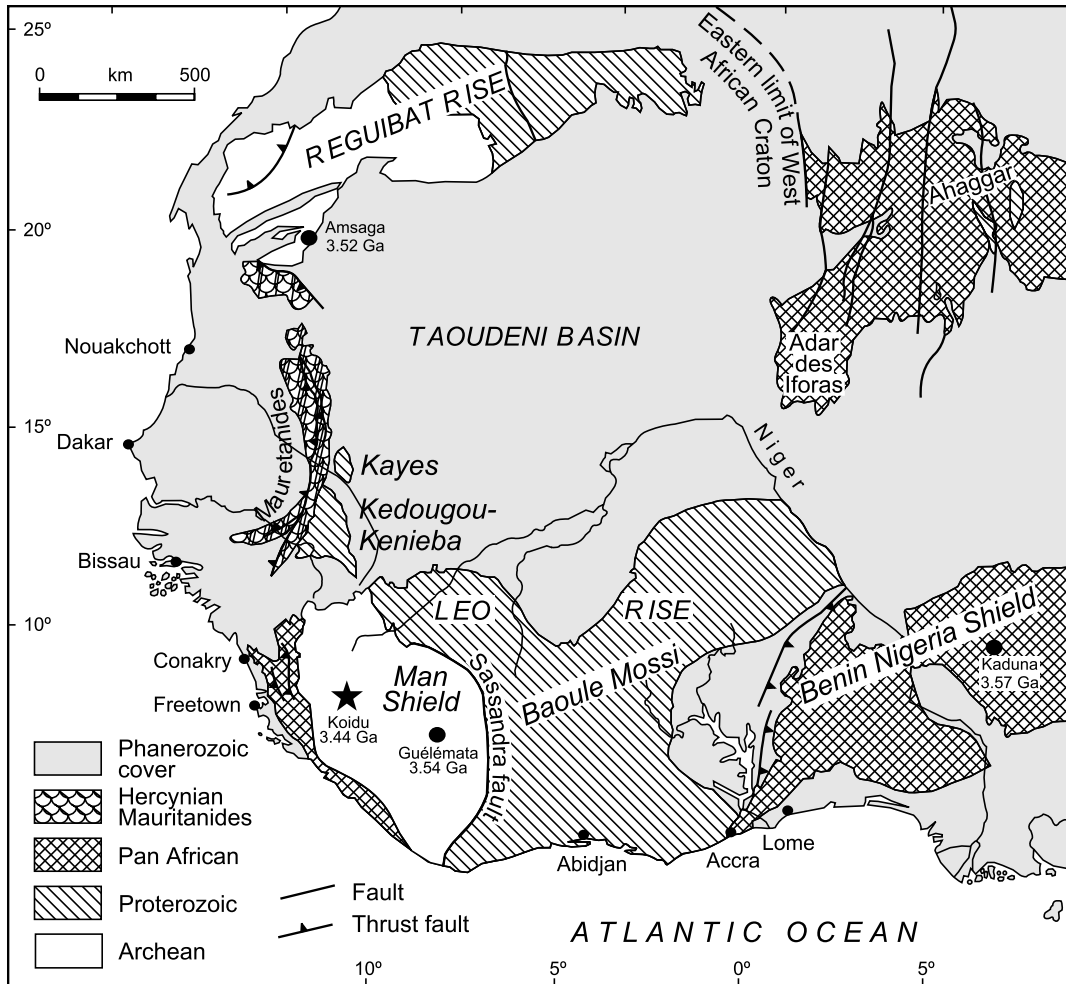


Fig. 1. Major tectonic units of the West African craton (Boher et al., 1992) showing the locations of the Koidu kimberlite complex (star, age of the low MgO eclogite suite) and of Early Archean crustal rocks in West Africa (solid circles): Guélématata orthogneiss, Mount Nimba hills, Guinea (Thiéblemont et al., 2001), the Amsaga area, Reguibat Rise (Potrel et al., 1996), and Kaduna, northern Nigeria (Kröner et al., 2001).

the Reguibat Rise (Potrel et al., 1996, 1998; see Fig. 1).

The Man Shield, the Archean part of the Leo Rise, has been divided into three age provinces (Macfarlane et al., 1981): Leonean (~ 3.0 Ga), Liberian (~ 2.7 Ga), and Eburnian (~ 2.0 Ga). Due to limited radiometric dating (Rb–Sr and Pb–Pb whole rock), there is debate as to whether the Leonean and Liberian are two separate events or a single, long-lived event (Williams, 1978). Recent SHRIMP zircon ages (~ 3.5 Ga) in the Mount Nimba hills of Guinea (Thiéblemont et al.,

2001; see Fig. 1) and earlier, poorly constrained Rb–Sr studies (Hedge et al., 1975; Hurley et al., 1975) and Nd model ages (Kouamelan et al., 1997) point toward a pre-Leonian crustal growth event (> 3.2 Ga). A younger Pan-African age province defines a tectonic event at ~ 550 Ma in the coastal belt of Sierra Leone and Liberia.

The Archean basement (Leonean and Liberian provinces) of Sierra Leone is typical of granite–greenstone terrains found in ancient continental nuclei. Older TTG gneisses (~ 3 Ga, Beckinsale et al., 1980) form between 60 and 70% of the outcrop

area and are the major rock type of the Man Shield. Younger granites (2.7–2.8 Ga) intrude the margins of the greenstone belts or occur as thick sheets cross-cutting the greenstones at high structural levels.

Little previous geochronological work has been done on the eclogitic xenoliths. Hills and Haggerty (1989) report two-point Sm–Nd mineral isochron ages for several of the Koidu eclogites ranging from 92 to 247 Ma. The equilibration temperatures of the Koidu eclogites (typically > 900 °C) exceed the closure temperature of the Sm–Nd system (600–700 °C; Harrison and Wood, 1980; Mezger et al., 1992). Thus, the relatively young Sm–Nd ages for the Koidu eclogites are most likely apparent ages without geological significance (Hills and Haggerty, 1989).

3. Sample description

Zircon separates of sample ‘old gneiss 278’ representing the older basement were provided by Dr Hugh Rollinson. The gneiss was collected in Motema Quarry at Yengema (sheet 58, 782529), a few kilometer west of the main kimberlite outcrops. The gneiss dominates between the Nimini Hill greenstone belt in the west and the Gori Hills in the east and is the main gneiss type into which the kimberlites intruded. This gneiss is a composite migmatite with two main components: a gray, dioritic portion and a later, intrusive pink portion that is more granitic. The gneiss also contains amphibolitic inclusions. Granulite xenolith KGR 86-75 from the Koidu kimberlite complex, Sierra Leone, consists of garnet, pyroxene, and plagioclase with accessory rutile. Petrography, whole rock and mineral major element data are given in Hills and Haggerty (1989). Zircons in KGR 86-75 were probed in thin section.

Hills and Haggerty (1989) and Barth et al. (2001, 2002) describe the petrography and report whole rock and mineral chemical data for the Koidu eclogite samples analyzed for Re–Os. The high MgO group is essentially bi-mineralic, with only minor ilmenite, and/or sulfide occurring in addition to garnet and omphacite. The low MgO group commonly contains accessory phases such

as kyanite, graphite, quartz (after coesite), diamond, amphibole, and/or corundum plus rutile, and/or sulfides in addition to garnet and omphacite.

Whole rock powders originally were prepared by crushing in steel jaw crushers and tungsten carbide for XRF measurement (cf. Hills and Haggerty, 1989). In some cases, where enough material was available, new whole rock powders were prepared by crushing in alumina ceramics (see Table 3). Powders processed both ways were analyzed for one sample (KEC 86-107) to determine whether contamination occurred during steel/tungsten carbide crushing.

4. Analytical methods

4.1. Zircon U/Pb isotopic measurement

U/Pb zircon isotopic data were determined by simultaneous solution nebulization and laser ablation (LA-) ICP-MS (Horn et al., 2000). Ablation is achieved by a 193 nm Ar–F excimer laser system using a pulse repetition rate of 10 Hz and pulse energy of ≤ 0.5 mJ (Horn et al., 2000). Typically, a ~ 50 μm spot diameter was used. Analyses were performed on a Fisons (VG Elemental) PQ II+ in pulse counting mode (one point per peak); dwell time and quadrupole settling time were set to 10 and 5 ms, respectively. Data reduction follows the procedures outlined in Longerich et al. (1996) and Horn et al. (2000). The time-resolved spectra were processed off-line using a spreadsheet program to apply the background subtraction and mass discrimination, fractionation, interference, and common lead corrections (modified version of LAMTRACE© by Simon Jackson). For the common Pb correction, we used the 3 Ga common Pb of Stacey and Kramers (1975). Zircon 91 500 and Phalaborwa baddeleyite were measured to monitor accuracy. Measurement of zircon 91 500 yielded a weighted mean $^{207}\text{Pb}/^{206}\text{Pb}$ age of 1093 ± 30 Ma (2σ , $n = 12$; TIMS age 1062.4 ± 0.8 Ma, Wiedenbeck et al., 1995). Phalaborwa baddeleyite yielded an upper intercept age of 2057 ± 28 Ma and a weighted mean $^{207}\text{Pb}/^{206}\text{Pb}$ age of 2068 ± 21 Ma ($n = 4$; TIMS ages 2060.5 ± 1.9 and 2060.2 ± 2.1

Ma, respectively, Reischmann, 1995). Concordia intercepts and weighted mean ages reported in this study were calculated in the program ISOPLOT/EX of Ludwig (1998). Errors are given at the 2σ or 95% confidence level.

4.2. Re/Os chemistry and measurement

Rhenium and osmium isotopic compositions were determined on whole rock eclogites following the procedures described in Carlson et al. (1999). Dissolutions were performed in Carius tubes to overcome problems of spike-sample equilibration (Shirey and Walker, 1995). A mixed spike with ^{190}Os and ^{185}Re was added prior to digestion with reverse aqua regia. Os was extracted with CCl_4 and then back extracted into concentrated HBr. The Os containing HBr was dried, then dissolved in H_2SO_4 using CrO_3 as an oxidant, from which the Os was distilled at 90°C , and trapped into HBr (Roy-Barman and Allègre, 1994). The Re-containing solution remaining after Os extraction was dried, then taken up in 1 N HCl and centrifuged to remove solids. Re was separated by anion exchange using 1 ml of AG-1 X8 resin, Re being eluted with 4 N HNO_3 . Re was further purified using a second, smaller column.

Rhenium and Osmium were run as ReO_4^- and PsP_3^- ions by negative thermal ionization mass spectrometry (N-TIMS) on the DTM 15 in. radius mass spectrometer, generally following procedures outlined by Pearson et al. (1995a). Both Re and Os were loaded onto single Pt filaments using $\text{Ba}(\text{NO}_3)_2$ as an electron donor. Os isotope compositions are corrected for mass dependent isotope fractionation by normalizing to $^{192}\text{Os}/^{188}\text{Os} = 3.082614$.

5. Results

5.1. U–Pb dating of ‘old gneiss 278’

Zircons in sample ‘old gneiss 278’ are dominated by transparent to brownish prismatic grains with slightly etched rims. Grains show internal structures ranging from oscillatory zoning in cores, to cores with secondary phases (e.g. baddeleyite,

determined by semiquantitative EDS) discordant with the original oscillatory zoning and rims with only faint traces of original oscillatory zoning (Fig. 2). Fine-scale oscillatory zoned grains are interpreted as having crystallized from a felsic magma (e.g. Poldervaart, 1956; Pidgeon et al., 1998). Following the recrystallization model of Pidgeon et al. (1998), grains with weakly zoned rims and cores with cross-cutting secondary phases are the result of decomposition of zircon during cooling of felsic magma or during metamorphism. Decomposition of zircon results in the formation of a stable low trace element zircon phase around the rim of the zircon and the relocation of expelled trace elements to concentrate in one or two bands, located initially along primary zones, towards the center of the grain (Pidgeon et al., 1998).

Ages determined from prismatic zircons with oscillatory zoning parallel to grain exteriors, devoid of inherited cores and without younger shells of oscillatory zoned zircon give an igneous age for quartzo-feldspathic meta-igneous rocks (e.g. Nutman et al., 2000). The recrystallized outer rims of zircons with only faint traces of oscillatory zoning might record the time interval between primary crystallization and the onset of zircon decomposition during cooling of the igneous body, the age of metamorphism, or an unresolvable mixed age (Pidgeon et al., 1998).

Single spot LA-ICP-MS zircon analyses are presented in Table 1. Zircons are discordant to slightly reverse discordant (excess radiogenic Pb or loss of U, Fig. 3). The analyses do not define a single discordance line within analytical uncertainties (MSWD = 6.9). The concordia intercepts calculated are 2890 ± 9 Ma and 210 ± 47 Ma (Fig. 3). The $^{207}\text{Pb}/^{206}\text{Pb}$ ratios give ages up to, and even slightly above (the maximum $^{207}\text{Pb}/^{206}\text{Pb}$ age is 2944 ± 13 Ma), the concordia intersection age. The weighted mean $^{207}\text{Pb}/^{206}\text{Pb}$ age is 2877 ± 10 Ma ($n = 53$).

Low count rates on ^{204}Pb combined with an interference correction for ^{204}Hg result in limited precision for the common Pb correction, which may cause some of the scatter of the $^{207}\text{Pb}/^{206}\text{Pb}$ ages. Although the presence of multiple generations of zircons cannot be excluded, the range of internal structures combined with the discordance

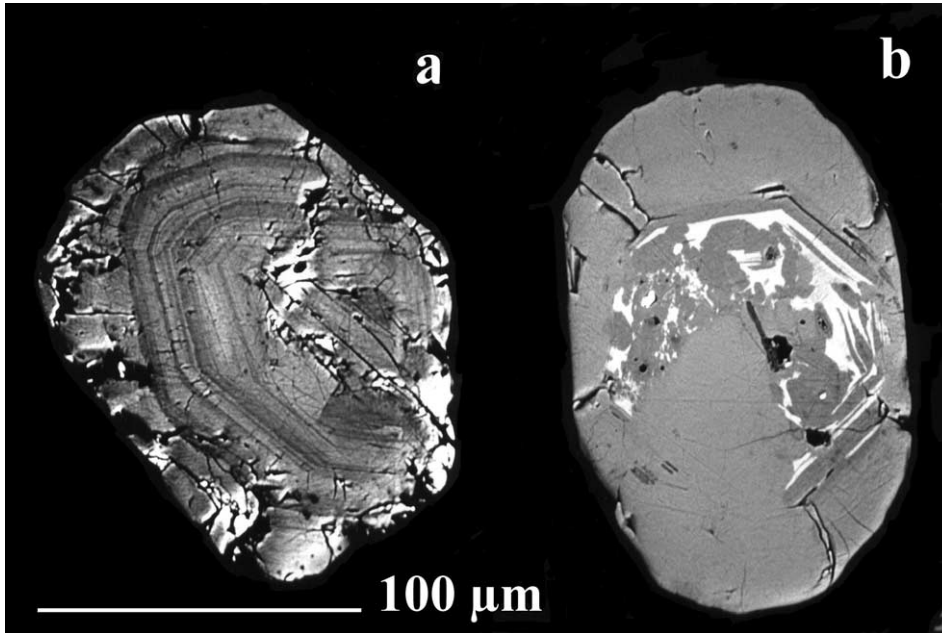


Fig. 2. Back scattered electrons (BSE) images of two zircon grains in tonalitic gneiss sample 'old gneiss 278'. (a) Grain with etched rim and preserved primary, fine-scale oscillatory zoning parallel to grain faces. (b) Grain with pale, recrystallized rim with only faint traces of oscillatory zoning and with secondary phases (baddeleyite) discordant to original oscillatory zoning in the core. Grain sizes $\sim 100 \mu\text{m}$.

pattern of the zircons is consistent with all zircons having the same age, but having responded very differently to later isotopic disturbance. The internal structure of the pale rims (open symbols, Fig. 3), which are interpreted as the survival of ghost euhedral zoning, leaves little doubt that the rims are recrystallization products of a later metamorphism rather than being new zircon growth. Due to the grain size of the zircons ($< 150 \mu\text{m}$) and the relatively large spot sizes used ($50\text{--}60 \mu\text{m}$), separate core and rim measurements could only be made in a few cases. Rims have similar $^{207}\text{Pb}/^{206}\text{Pb}$ ratios to the cores but higher U/Pb ratios, suggestive of recent Pb loss (Table 1). Analyses that fall off the discordance line towards younger ages probably reflect mixed ages between the time of crystallization of the igneous protolith and the time of metamorphism. Therefore, the youngest $^{207}\text{Pb}/^{206}\text{Pb}$ age of $2743 \pm 13 \text{ Ma}$ is a maximum age for metamorphism.

Xenocrystic cores were found in four zircon grains, distinguished by their significantly older $^{207}\text{Pb}/^{206}\text{Pb}$ ages. Optically and on BSE images the

cores are not obviously different from the rest of the population (cores are transparent to brownish, sometimes with oscillatory zoning or inclusions). Three of the four analyses fall on a discordance line with concordia intercepts at 3555 ± 57 and $343 \pm 240 \text{ Ma}$ (Fig. 4).

5.2. U–Pb dating of granulite xenolith KGR 86-75

Zircons in granulite xenolith KGR 86-75 from the Koidu kimberlite complex occur as prismatic to rounded inclusions in garnet and plagioclase. Internal structures show only faint traces of oscillatory zoning. Due to the small grain size of most of the zircons ($25\text{--}70 \mu\text{m}$), and their low U content, only two grains could be measured by LA-ICP-MS (Table 2). The zircons are concordant and overlap in ages (Fig. 5). The zircon included in garnet has a $^{206}\text{Pb}/^{238}\text{U}$ age of $2674 \pm 35 \text{ Ma}$ and a $^{207}\text{Pb}/^{206}\text{Pb}$ age of $2707 \pm 29 \text{ Ma}$. The zircon included in plagioclase has a less precise $^{206}\text{Pb}/^{238}\text{U}$ age of $2759 \pm 86 \text{ Ma}$ and a $^{207}\text{Pb}/^{206}\text{Pb}$ age of $2843 \pm 124 \text{ Ma}$.

Table 1
Single spot LA-ICP-MS isotope ratio and age determinations of sample 'old gneiss 278'

Grain number	$^{206}\text{Pb}/^{238}\text{U}$	$\pm 2\sigma$	$^{207}\text{Pb}/^{235}\text{U}$	$\pm 2\sigma$	$^{207}\text{Pb}/^{206}\text{Pb}$	$\pm 2\sigma$	$^{206}\text{Pb}/^{238}\text{U}$ age	$^{207}\text{Pb}/^{235}\text{U}$ age	$^{207}\text{Pb}/^{206}\text{Pb}$ age
1	0.5204	0.0086	14.67	0.29	0.2055	0.0028	2701 ± 37	2794 ± 19	2870 ± 22
2, core	0.4589	0.0061	13.21	0.22	0.2100	0.0026	2435 ± 27	2695 ± 16	2905 ± 20
2, rim	0.4119	0.0076	11.64	0.23	0.2069	0.0020	2223 ± 35	2576 ± 18	2881 ± 16
3	0.3548	0.0082	10.29	0.26	0.2116	0.0026	1957 ± 39	2461 ± 24	2918 ± 20
4, rim	0.2537	0.0036	6.82	0.11	0.1964	0.0019	1457 ± 18	2088 ± 15	2796 ± 16
4, core	0.4571	0.0060	12.90	0.18	0.2066	0.0026	2427 ± 26	2673 ± 13	2879 ± 20
5, core	0.3616	0.0062	9.92	0.19	0.2004	0.0019	1990 ± 29	2427 ± 17	2829 ± 15
5, rim	0.3224	0.0058	8.87	0.18	0.2009	0.0020	1801 ± 28	2324 ± 18	2833 ± 16
6	0.5139	0.0082	14.97	0.24	0.2136	0.0028	2673 ± 35	2813 ± 15	2933 ± 21
7	0.4145	0.0064	11.72	0.21	0.2064	0.0026	2235 ± 29	2582 ± 16	2877 ± 20
8	0.2990	0.0046	8.17	0.14	0.1993	0.0024	1686 ± 23	2250 ± 16	2821 ± 20
9	0.2763	0.0055	7.39	0.16	0.1958	0.0020	1573 ± 28	2159 ± 19	2791 ± 16
10	0.5214	0.0083	14.99	0.26	0.2107	0.0028	2705 ± 35	2814 ± 16	2911 ± 21
11, rim	0.4589	0.0060	13.17	0.20	0.2098	0.0018	2434 ± 27	2692 ± 14	2904 ± 14
11, core	0.5026	0.0150	14.09	0.44	0.2050	0.0028	2625 ± 65	2756 ± 30	2867 ± 22
12	0.4994	0.0081	14.11	0.30	0.2066	0.0031	2611 ± 35	2757 ± 20	2879 ± 24
13	0.5315	0.0063	14.90	0.25	0.2050	0.0024	2748 ± 27	2809 ± 16	2866 ± 19
14	0.4759	0.0090	13.39	0.29	0.2057	0.0029	2509 ± 39	2707 ± 20	2872 ± 23
15, rim	0.5018	0.0063	14.31	0.23	0.2087	0.0030	2621 ± 27	2771 ± 15	2896 ± 23
16	0.2054	0.0069	5.33	0.20	0.1901	0.0015	1204 ± 37	1873 ± 32	2743 ± 13
17	0.4239	0.0051	11.89	0.16	0.2048	0.0015	2278 ± 23	2596 ± 12	2865 ± 12
18	0.4496	0.0081	12.77	0.24	0.2080	0.0019	2393 ± 36	2663 ± 18	2890 ± 15
19	0.5099	0.0081	14.33	0.26	0.2056	0.0021	2656 ± 35	2772 ± 17	2871 ± 16
20	0.4252	0.0081	12.14	0.29	0.2082	0.0034	2284 ± 36	2616 ± 22	2892 ± 26
21	0.4936	0.0048	14.26	0.16	0.2115	0.0014	2586 ± 21	2767 ± 11	2917 ± 11
22	0.3746	0.0110	10.45	0.33	0.2036	0.0046	2051 ± 51	2476 ± 29	2855 ± 36
23	0.4141	0.0055	11.64	0.15	0.2056	0.0016	2233 ± 25	2576 ± 12	2871 ± 12
24	0.4373	0.0067	12.41	0.26	0.2072	0.0029	2339 ± 30	2636 ± 20	2884 ± 23
25	0.4991	0.0082	14.24	0.33	0.2086	0.0028	2610 ± 35	2766 ± 22	2895 ± 21
26	0.4524	0.0062	12.74	0.24	0.2061	0.0026	2406 ± 28	2661 ± 18	2875 ± 20
27	0.3706	0.0120	10.19	0.34	0.2012	0.0021	2032 ± 57	2452 ± 31	2836 ± 17
28	0.5917	0.0116	16.63	0.42	0.2055	0.0040	2996 ± 47	2914 ± 24	2870 ± 32
29	0.5057	0.0047	14.89	0.18	0.2151	0.0018	2638 ± 20	2808 ± 11	2944 ± 13
30	0.4956	0.0063	14.11	0.21	0.2080	0.0023	2595 ± 27	2757 ± 14	2890 ± 18
31	0.5217	0.0064	14.75	0.33	0.2069	0.0040	2706 ± 27	2799 ± 21	2881 ± 31
32	0.5008	0.0095	14.44	0.41	0.2107	0.0046	2617 ± 41	2779 ± 27	2911 ± 36
33	0.5469	0.0097	14.90	0.49	0.1983	0.0058	2812 ± 41	2809 ± 31	2812 ± 48
34	0.4339	0.0086	12.55	0.25	0.2113	0.0024	2323 ± 39	2646 ± 18	2915 ± 18
35	0.5617	0.0072	15.61	0.35	0.2034	0.0037	2874 ± 30	2853 ± 21	2853 ± 29
36	0.2451	0.0043	6.61	0.15	0.1971	0.0047	1413 ± 22	2060 ± 20	2803 ± 39
37	0.2385	0.0029	6.43	0.10	0.1971	0.0017	1379 ± 15	2037 ± 13	2803 ± 14
38	0.4452	0.0064	12.73	0.27	0.2091	0.0030	2374 ± 29	2660 ± 20	2899 ± 24
39	0.4371	0.0063	12.44	0.17	0.2088	0.0017	2338 ± 28	2638 ± 13	2896 ± 13
40	0.3576	0.0066	10.11	0.35	0.2065	0.0060	1971 ± 31	2445 ± 32	2878 ± 47
41	0.5098	0.0057	14.56	0.28	0.2091	0.0033	2656 ± 24	2787 ± 18	2899 ± 26
42	0.4693	0.0045	13.22	0.17	0.2062	0.0019	2480 ± 20	2696 ± 12	2876 ± 15
43	0.4985	0.0076	14.17	0.32	0.2080	0.0036	2608 ± 33	2761 ± 21	2890 ± 28
44	0.4978	0.0194	13.90	0.72	0.2044	0.0057	2604 ± 84	2743 ± 49	2862 ± 46
45	0.6199	0.0128	17.14	0.44	0.2021	0.0029	3110 ± 51	2943 ± 25	2843 ± 23
46	0.3729	0.0065	10.37	0.25	0.2032	0.0034	2043 ± 31	2469 ± 23	2852 ± 27
47	0.5058	0.0086	13.88	0.42	0.2012	0.0048	2639 ± 37	2742 ± 29	2836 ± 39
48	0.5486	0.0075	15.49	0.30	0.2065	0.0033	2820 ± 31	2846 ± 19	2878 ± 26

Table 1 (Continued)

Grain number	$^{206}\text{Pb}/^{238}\text{U}$	$\pm 2\sigma$	$^{207}\text{Pb}/^{235}\text{U}$	$\pm 2\sigma$	$^{207}\text{Pb}/^{206}\text{Pb}$	$\pm 2\sigma$	$^{206}\text{Pb}/^{238}\text{U}$ age	$^{207}\text{Pb}/^{235}\text{U}$ age	$^{207}\text{Pb}/^{206}\text{Pb}$ age
49	0.4973	0.0068	14.25	0.24	0.2098	0.024	2602 ± 29	2766 ± 16	2904 ± 18
<i>Xenocrystic cores</i>									
15, core	0.6389	0.0136	27.81	0.69	0.3183	0.0040	3185 ± 54	3412 ± 24	3562 ± 19
50	0.4460	0.0071	18.49	0.31	0.3036	0.0020	2378 ± 32	3016 ± 16	3489 ± 10
51	0.4027	0.0056	14.18	0.28	0.2575	0.0030	2182 ± 26	2762 ± 18	3232 ± 18
52	0.3778	0.0075	15.61	0.36	0.3019	0.0027	2066 ± 35	2853 ± 22	3480 ± 14

5.3. Re–Os dating of the Koidu eclogite suite

Re and Os abundances and $^{187}\text{Re}/^{188}\text{Os}$ and $^{187}\text{Os}/^{188}\text{Os}$ isotopic compositions of the Koidu eclogites are given in Table 3 and in Figs. 6 and 7. Re and Os concentrations for the separately processed splits of sample KEC 86-107 are ~ 3 and $\sim 40\%$ lower and $^{187}\text{Re}/^{188}\text{Os}$ is $\sim 50\%$ higher in the steel/tungsten carbide-processed split than in the alumina ceramics-processed split (Table 3). These differences are most likely due to nugget effects (i.e. heterogeneous distribution of Re- and

Os-bearing trace phases such as sulphides) since any contamination from the WC mill or steel jaw crusher would result in higher Re and Os concentrations in those samples processed in this fashion, which is opposite to observation. However, nugget effects may potentially mask the effect of contamination during crushing. While we cannot rule out that some of the steel/tungsten carbide-processed samples have been compromised, our analyses of sample KEC 86-107 suggest that crushing did not have a significant impact on the Re–Os results for samples processed in steel-WC.

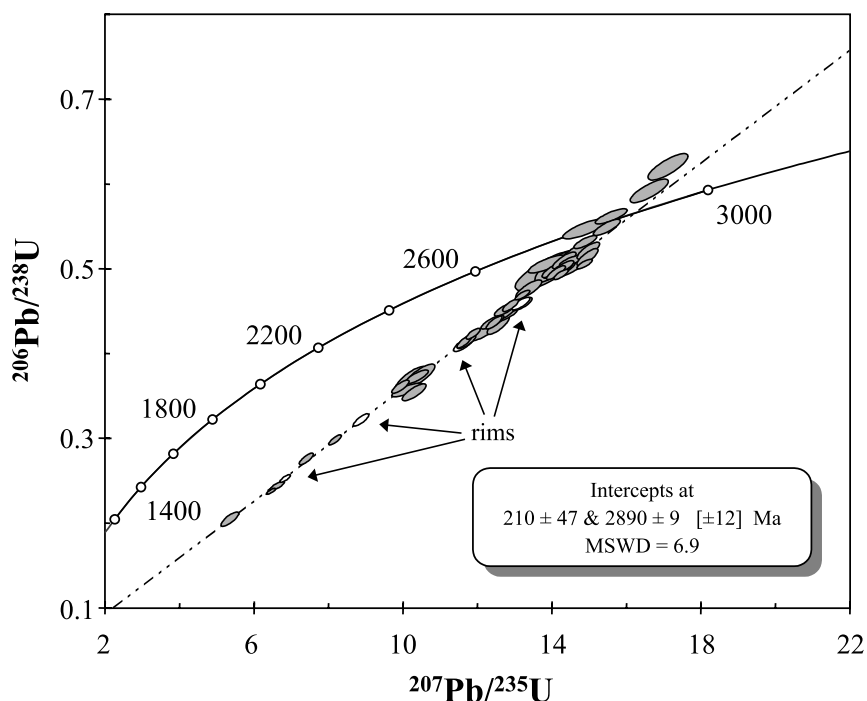


Fig. 3. Concordia diagram showing results for sample 'old gneiss 278' with spots ranging from discordant to reverse discordant. Age uncertainty in square brackets includes decay constant errors. Open ellipses: rim analyses. Error ellipses are 2σ .

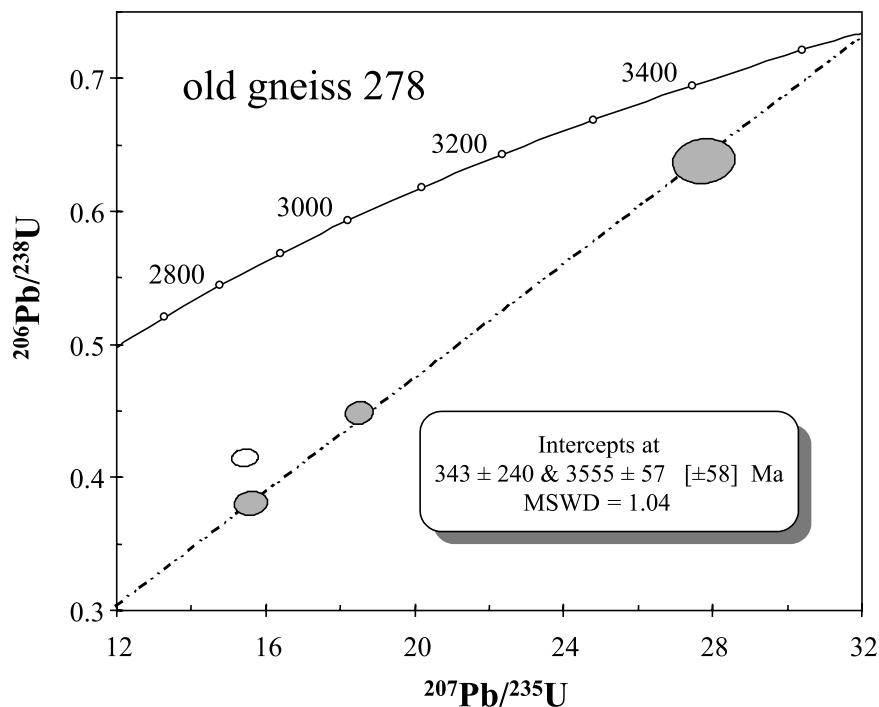


Fig. 4. Concordia diagram showing results for xenocrystic cores of sample 'old gneiss 278'. Age uncertainty in square brackets includes decay constant errors. Open ellipse: xenocrystic core (spot 51) that has a younger $^{207}\text{Pb}/^{206}\text{Pb}$ age than the other three cores and does not fall on the same discordance line. Error ellipses are 2σ .

Both low MgO and high MgO eclogites have a wide range of Re and Os contents (0.02–3.4 ppb Re and 0.026–2.2 ppb Os, Fig. 6). All samples have superchondritic $^{187}\text{Re}/^{188}\text{Os}$ (2.2–93) and $^{187}\text{Os}/^{188}\text{Os}$ (0.22–8.8). By comparison, the Koidu eclogites have a similar range of Re and Os abundances and Re–Os isotopic compositions to eclogite xenoliths from Udachnaya, Siberia (Pearson et al., 1995b) and a wider range than eclogite xenoliths from the Newlands kimberlite, South Africa (Menzies et al., 1998; Shirey et al., 2001).

The $^{187}\text{Re}/^{188}\text{Os}$ versus $^{187}\text{Os}/^{188}\text{Os}$ systematics of the eclogites (Fig. 7) show considerable scatter, defining no statistically significant isochrons. The

scatter is most pronounced among the high MgO samples (Fig. 7b), and may be due to disturbance of the Re–Os system or reflect multiple generations of eclogites. Eleven out of 13 of the low MgO samples scatter about a line with slope corresponding to an age of 3.44 ± 0.76 Ga (2σ), which is consistent with an Archean origin for the protoliths of these eclogites.

The scatter of the Re–Os data could also be caused by infiltration of the eclogites by kimberlitic melts. Like most eclogite xenoliths, the Koidu samples show abundant evidence for interaction with kimberlite (Hills and Haggerty, 1989; Fung and Haggerty, 1995; Barth et al., 2001, 2002).

Table 2

Single spot LA-ICP-MS isotope ratio and age determinations of granulite xenolith KGR 86-75

Grain number	$^{206}\text{Pb}/^{238}\text{U}$	$\pm 2\sigma$	$^{207}\text{Pb}/^{235}\text{U}$	$\pm 2\sigma$	$^{207}\text{Pb}/^{206}\text{Pb}$	$\pm 2\sigma$	$^{206}\text{Pb}/^{238}\text{U}$ age	$^{207}\text{Pb}/^{235}\text{U}$ age	$^{207}\text{Pb}/^{206}\text{Pb}$ age
1, in garnet	0.5140	0.0083	13.07	0.35	0.1859	0.0033	2674 ± 35	2684 ± 25	2707 ± 29
2, in plagioclase	0.5341	0.0204	14.70	1.00	0.2021	0.0154	2759 ± 86	2796 ± 65	2843 ± 124

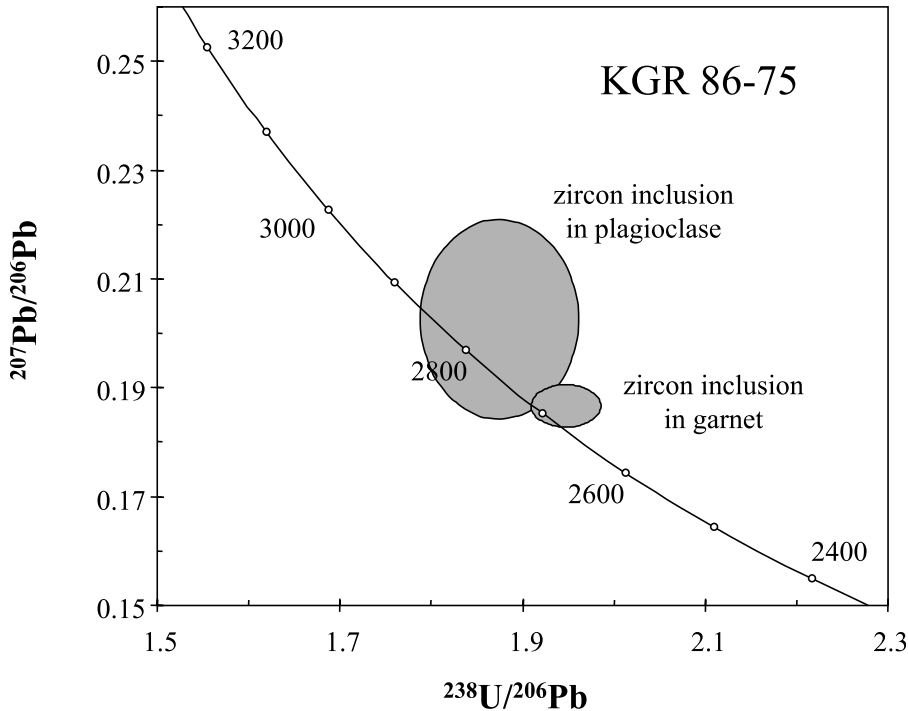


Fig. 5. Tera–Wasserburg concordia diagram (Tera and Wasserburg, 1972) showing individual spot analyses of zircons in granulite xenoliths KGr 86-75. Large gray ellipse: zircon inclusion in plagioclase. Small gray ellipse: zircon inclusion in garnet. Error ellipses are 2σ .

Most analyses of kimberlites have yielded Re/Os ratios that are similar or lower than those of the eclogites and much lower $^{187}\text{Os}/^{188}\text{Os}$ (Walker et al., 1989; Carlson et al., 1999; Graham et al., 1999). Both of these effects should cause the Re–Os model ages to diverge to model ages that are too young.

The eclogites exhibit a wide range of Re–Os mantle model ages (Table 3). For the high MgO samples, more than half of the Re–Os model ages are older than the age of the Earth, indicating they either experienced recent Re loss or gain of radiogenic Os. Considering their mantle origin and the limited range of $^{187}\text{Os}/^{188}\text{Os}$ observed in mantle samples, the former seems more likely than the latter. Five out of 13 of the low MgO samples also have Re–Os model ages older than the Earth. However, six of the remaining samples show a relatively limited span in Re–Os model ages, ranging from 3.06 to 3.95 Ga, again suggestive of

an Archean formation age for the protoliths of these eclogites.

6. Geological implications

6.1. Evolution of the Archean basement in Sierra Leone

The oldest zircons in sample ‘old gneiss 278’ are the xenocrystic cores, documenting the presence of an Early Archean (3.5–3.6 Ga) component in the basement of Sierra Leone. This age overlaps the oldest zircon ages reported from the Mount Nimba hills of Guinea (3.5 Ga; Thiéblemont et al., 2001), the Amsaga area, Reguibat Rise (3.5 Ga; Potrel et al., 1996), and from northern Nigeria (3.57 Ga; Kröner et al., 2001), demonstrating that such Early Archean components are widespread in parts of West Africa (Fig. 1).

Table 3

MgO content, Re–Os abundances, and Re–Os isotopic compositions of Koidu eclogite xenoliths (all samples have KEC prefix)

Sample	MgO (wt. %)	Re (ppb)	Os (ppb)	$^{187}\text{Re}/^{188}\text{Os}$	$^{187}\text{Os}/^{188}\text{Os}$	T_{BE} (Ga)
<i>Low MgO eclogites</i>						
81-3	9.24	0.506 ± 0.001	0.0597 ± 0.0010	51.43 ± 0.88	2.106 ± 0.042	2.28
81-4	12.56	1.01 ± 0.01	0.404 ± 0.004	13.29 ± 0.03	0.934 ± 0.002	3.64
81-5w	10.35	0.0914 ± 0.0005	0.191 ± 0.001	2.368 ± 0.019	0.326 ± 0.001	5.80
81-7	12.96	0.909 ± 0.004	0.919 ± 0.014	5.163 ± 0.007	0.767 ± 0.001	7.58
81-8	10.08	1.06 ± 0.01	0.0934 ± 0.0010	93.37 ± 0.96	5.493 ± 0.094	3.37
81-10A	11.44	0.893 ± 0.001	0.129 ± 0.002	50.70 ± 0.40	4.140 ± 0.048	4.61
81-18	12.01	0.707 ± 0.001	0.0911 ± 0.0011	80.14 ± 0.93	8.833 ± 0.218	6.22
81-21	12.16	2.23 ± 0.02	0.415 ± 0.002	31.95 ± 0.08	1.917 ± 0.005	3.31
86-13w	10.14	0.808 ± 0.001	0.0769 ± 0.0010	92.14 ± 1.21	6.362 ± 0.150	3.95
86-71Aw	10.08	0.197 ± 0.001	0.443 ± 0.005	2.174 ± 0.007	0.220 ± 0.000	3.07
86-72Aw	7.09	3.39 ± 0.001	0.354 ± 0.001	67.84 ± 0.20	3.717 ± 0.015	3.11
86-72Bw	9.50	0.781 ± 0.001	0.0353 ± 0.0010	158.5 ± 4.5	3.829 ± 0.162	1.39
86-74Bw	6.19	0.116 ± 0.0005	0.0259 ± 0.0010	28.65 ± 1.06	2.662 ± 0.127	5.16
<i>High MgO eclogites</i>						
81-2	16.68	0.0200 ± 0.0005	0.0553 ± 0.0010	3.716 ± 0.115	8.742 ± 0.344	77.16
81-11	19.51	2.73 ± 0.029	2.23 ± 0.03	6.362 ± 0.003	0.713 ± 0.000	5.64
86-15w	15.90	0.611 ± 0.001	0.0778 ± 0.0010	56.18 ± 0.7418	3.808 ± 0.072	3.84
86-19w	16.29	0.358 ± 0.0005	0.0715 ± 0.0010	46.17 ± 0.63	7.108 ± 0.184	8.52
86-58w	19.62	0.140 ± 0.001	0.464 ± 0.004	1.476 ± 0.006	0.221 ± 0.000	5.07
86-73Aw	17.65	0.0486 ± 0.0005	0.0561 ± 0.0010	4.899 ± 0.101	1.448 ± 0.027	15.51
86-90w	18.13	1.374 ± 0.001	0.107 ± 0.001	90.46 ± 0.85	3.655 ± 0.048	2.31
86-107	20.15	0.480 ± 0.002	0.330 ± 0.001	7.406 ± 0.022	0.572 ± 0.001	3.69
86-107w	20.15	0.464 ± 0.001	0.201 ± 0.001	11.91 ± 0.06	0.674 ± 0.002	2.79

MgO contents from Hills and Haggerty (1989). Errors are calculated at the 2σ level either from blank correction or mass spectrometry (whichever is greater). Blank corrections were made for all data in the table. Sample 86-107 and 86-107w are two powders prepared from different parts of the same xenolith. Samples were crushed in alumina ceramics except samples with the suffix w (processed in steel jaw crushers and tungsten carbide). Os model ages (T_{BE}) are based on derivation from a chondritic reservoir using a ^{187}Re decay constant of 1.666×10^{-11} per year, $(^{187}\text{Os}/^{188}\text{Os})_{\text{BE}} = 0.1287$, and $(^{187}\text{Re}/^{188}\text{Os})_{\text{BE}} = 0.4243$.

The ages of zircons in sample ‘old gneiss 278’ that show no inherited cores, although scattered and showing in some cases a small amount of excess radiogenic Pb, form a coherent group with concordia intercepts at 2890 ± 9 and 210 ± 47 Ma. The fact that the analyses do not lie on a discordia line within analytical uncertainty suggests that their discordance was produced by at least two events, both older and younger than 210 Ma. Thus, the lower intercept probably has no direct age significance. The younger event is most likely zero-age Pb loss due to weathering and erosion of the grey gneiss. The older event is probably the Liberian event at 2.7 Ga, consistent with the youngest $^{207}\text{Pb}/^{206}\text{Pb}$ age of 2743 ± 13 Ma in the zircon population, which is interpreted to be a maximum age for metamorphism.

Two spot analyses show reverse discordance, i.e. excess radiogenic Pb. The fact that the disturbance of the Pb isotopic system generated local excesses of radiogenic Pb complicates the interpretation of the data by removing the constraint on crystallization age normally imposed by the $^{207}\text{Pb}/^{206}\text{Pb}$ apparent ages. The abnormal enrichment of ^{207}Pb in the excess Pb due to its early separation from its parent elements (possibly at 2.7 Ga) means that areas where excess Pb is present give $^{207}\text{Pb}/^{206}\text{Pb}$ apparent ages that geologically are too old (cf. Black et al., 1986; Corfu, 2000). To determine the minimum age for the zircon population it is, therefore, incorrect to use the maximum $^{207}\text{Pb}/^{206}\text{Pb}$ age measured (2944 ± 13 Ma). The most accurate age for the zircon population is probably given by the upper concordia intersec-

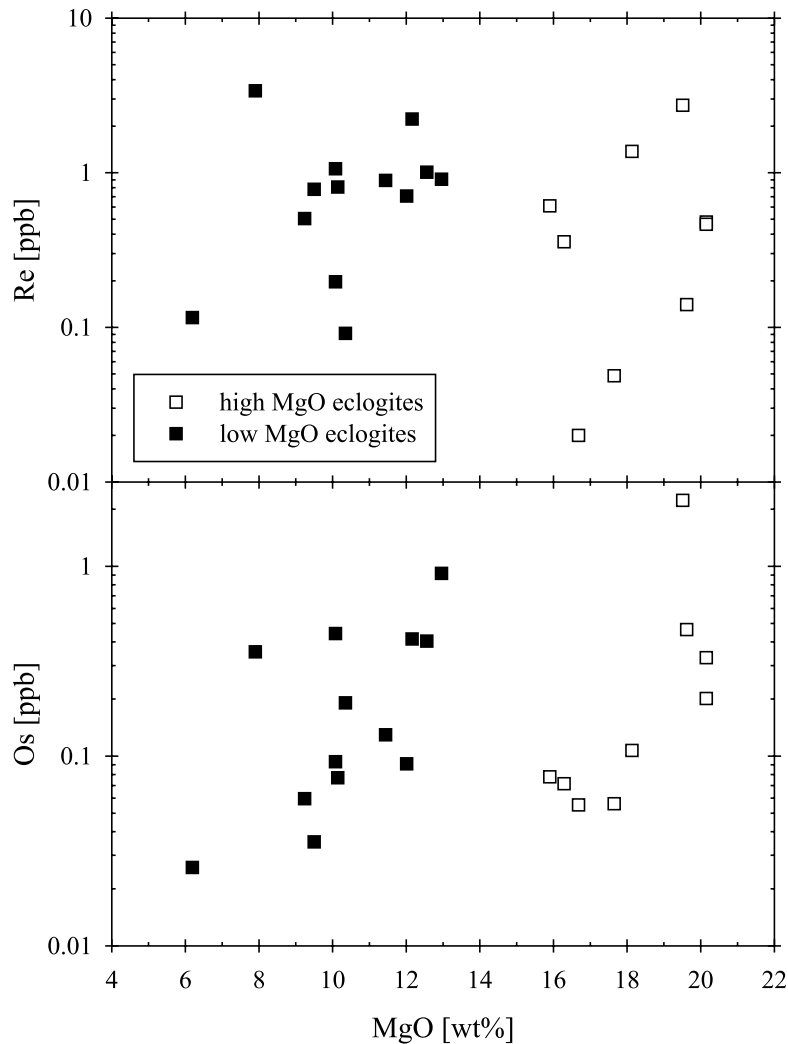


Fig. 6. Plot of whole rock MgO content vs. Re (top) and Os (bottom) concentration of Koidu eclogites. Open squares: high MgO eclogites. Solid squares: low MgO eclogites.

tion of 2890 ± 9 Ma, which is identical, within uncertainty, with the weighted mean $^{207}\text{Pb}/^{206}\text{Pb}$ age of 2877 ± 10 Ma.

The emplacement of the igneous protolith at 2890 ± 9 Ma is slightly younger than the Leonean Pb–Pb whole rock age of 2959 ± 50 Ma of a gneiss in the Fadugu district, Sierra Leone, determined by Beckinsale et al. (1980) and significantly younger than the Leonean crustal growth event identified in the Amsaga area, Reguibat Rise, of 2986 ± 8 Ma (Potrel et al., 1998). The emplacement

age is also younger than pre-Leonean to Leonean events recognized in western Côte d'Ivoire (3.0–3.2 Ga; Kouamelan et al., 1997). Thus, either the Leonean crustal growth event occurred later in Sierra Leone than in other parts of the West African Craton or the sample analyzed represents a separate, younger event. Sample 'old gneiss 278' is older than the 2.8 Ga event reported in Guinea (2797 ± 9 Ma; Thiéblemont et al., 2001) and western Côte d'Ivoire (Kouamelan et al., 1997; Cocherie et al., 1998). Hence, the period between

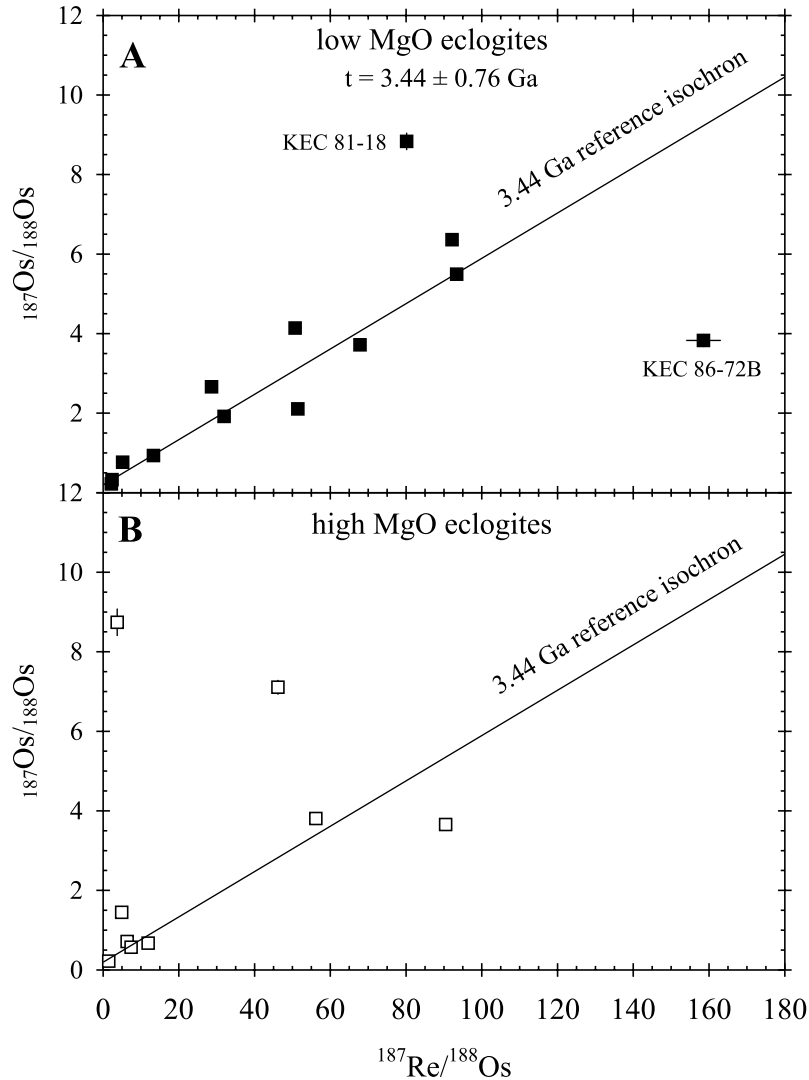


Fig. 7. Re–Os isochron plot of the Koidu low MgO (A) and high MgO (B) eclogites. Error bars are 2σ and are generally smaller than the symbols. Age in (A) calculated by regression of all low MgO eclogites except KEC 81-18 and KEC 86-72B.

the 3.0 Ga Leonean and the 2.7 Ga Liberian events appears to have included significant magmatic event(s).

The zircons in the granulite xenolith KGR 86-75 are concordant and their age is probably most accurately given by their mean weighted $^{206}\text{Pb}/^{238}\text{U}$ age of 2686 ± 32 Ma, which also coincides with the $^{207}\text{Pb}/^{206}\text{Pb}$ age of 2707 ± 29 Ma of the zircon inclusion in garnet. Based on the absence of igneous oscillatory zoning in the zircon

grains, this age is interpreted as the age of granulite-facies metamorphism. This metamorphic age represents the Liberian event and is consistent with the maximum age of metamorphism of 2743 ± 13 Ma derived from the grey gneiss.

The age of the Liberian event derived from the granulite xenolith is identical within uncertainty to the Rb–Sr whole rock age of 2753 ± 61 Ma of a gneiss in the Fadugu district, Sierra Leone (Beckinsale et al., 1980) and within the age range of

younger granites in Sierra Leone (2.7–2.8 Ga; Hurley et al., 1971; Rollinson and Cliff, 1982). The metamorphic age also agrees with 2.72 Ga monazite ages from western Côte d'Ivoire (Cocherie et al., 1998; interpreted to be recrystallization ages). It is, however, slightly younger than the Liberian age recognized in the Amsaga area, Reguibat Rise (2.73 Ga; Potrel et al., 1998) and significantly younger than the 2.8 Ga event in western Côte d'Ivoire (Kouamelan et al., 1997; Cocherie et al., 1998).

The zircons in the grey gneiss were relatively little affected by the high-grade metamorphism at 2.7 Ga. They were, however, strongly affected by zero-age Pb loss most likely caused by radiation damage coincident with uplift, weathering, and erosion. In contrast, the zircons analyzed in the granulite xenolith were strongly affected by the 2.7 Ga Liberian event but do not record zero-age Pb loss, consistent with U–Pb systematics in annealed zircons from other lower crustal xenoliths (e.g. Rudnick and Williams, 1987).

In summary, these rocks record the timing of three principal events in the history of the basement in Sierra Leone.

- 1) An initial crustal growth event in the Early Archean (3.5–3.6 Ga) is recorded in rare xenocrystic zircon cores from the gneiss.
- 2) Emplacement of the igneous precursor of the grey gneiss occurred at ca. 2.9 Ga, when most of the zircons crystallized.
- 3) High-grade lower crustal metamorphism during the Liberian event at 2.7 Ga, when the zircons in the granulite xenolith grew. The rims of some zircons in the grey gneiss recrystallized at the same time, presumably at a higher level in the crust.

6.2. Age of partial melting of the low MgO eclogites

The age of the eclogite facies metamorphism and partial melting is crucial for constraining the genetic relationship between the Koidu low MgO eclogites and the TTG. Unfortunately, the Re–Os results provide only limited constraints on this issue. Eleven out of 13 of the low-Mg eclogites

scatter about a line corresponding to 3.44 ± 0.76 Ga, consistent with the Re–Os systematics of these eclogites being established and/or last modified during the Archean. Only two samples give post-Archean Re–Os model ages. These two samples have among the lowest Os concentrations of the low-MgO samples analyzed, which makes them relatively sensitive to recent disturbance of the Re–Os system, for example, by infiltration by the host kimberlite. Whether the Re–Os systematics of the remainder of the samples reflects the original igneous protolith of these rocks or was induced during partial melting during eclogite formation is an interesting question, but not one that can be answered by the existing data. Since a reasonable maximum residence time for oceanic crust at Earth's surface is <200 Ma, the 760 Ma uncertainty of the Re–Os 'isochron' does not allow discrimination of the time between these events, both of which are likely to have affected the Re–Os system in the samples. While the Re–Os results are not sufficiently coherent to unambiguously tie the eclogite melting event to the time of TTG genesis in the Man Shield, the data do show that the most significant fractionation events in the history of the low-MgO eclogites occurred in the Archean. Thus, the data provide strong support for the idea that these eclogites were formed during Archean subduction. Furthermore, the data at least are consistent with the possibility that the chemical characteristics of these eclogites originated during construction of the TTG-rich Archean crust of the Man Shield.

6.3. Implications for Archean tectonics

Reliable formation ages for basement rocks in the Man Shield range from 2.9 to 3.2 Ga, with an Early Archean (3.5–3.6 Ga) crustal growth episode (see above). Though quite uncertain, the ~3.4 Ga Re–Os age for the eclogites suggests that formation of the eclogite protoliths, and their incorporation into the cratonic lithosphere, occurred during the earliest stages of growth of the Man Shield in the Archean. Chemical and oxygen isotope systematics indicate that the low MgO eclogites from the Koidu kimberlite complex are remnants of subducted oceanic crust that was

partially melted during subduction (Rollinson, 1997; Barth et al., 2001).

The 3.5 Ga Guélémeta orthogneiss samples analyzed by Thiéblemont et al. (2001) show characteristics of the complementary slab melts such as high Al₂O₃ (> 14.5%), SiO₂ (74%), Sr (> 320 ppm) and very low heavy REEs (e.g. < 0.3 ppm Yb) and Nb and Ta (< 2.5 and 0.15 ppm, respectively) contents. Thiéblemont et al. (2001) proposed 10–25% melting of a non-depleted basic protolith under eclogite facies conditions, which is in excellent agreement with the petrogenetic models for the Koidu low MgO eclogites put forward by Rollinson (1997) and Barth et al. (2001). We, therefore, suggest that the production of Archean TTG in the Man Shield was accomplished, in part, by melting of the protoliths of the materials now sampled as the Koidu eclogite xenoliths. If so, this suggests that Archean crustal growth in the Man Shield occurred in a convergent margin setting.

Acknowledgements

We thank Hugh Rollinson for zircon samples from the tonalite and Steve Haggerty for eclogite samples. We also thank David Lange for help with the SEM imaging. Reviews by S. Graham and J.J. Peucat helped to improve the manuscript. This study has been supported by NSF grants EAR 9804677 to R.L. Rudnick and EAR 9711008 to R.L. Rudnick and W.F. McDonough.

References

- Abouchami, W., Boher, M., Michard, A., Albarède, F., 1990. A major 2.1 Ga event of mafic magmatism in West Africa: an early stage of crustal accretion. *J. Geophys. Res.* 95, 17605–17629.
- Allègre, C.J., Luck, J.-M., 1980. Osmium isotopes as petrogenetic and geological tracers. *Earth Planet Sci. Lett.* 48, 148–154.
- Barth, M.G., Rudnick, R.L., Horn, I., McDonough, W.F., Spicuzza, M.J., Valley, J.W., Haggerty, S.E., 2001. Geochemistry of xenolithic eclogites from West Africa, part I: a link between low MgO eclogites and Archean crust formation. *Geochim. Cosmochim. Acta* 65, 1499–1527.
- Barth, M.G., Rudnick, R.L., Horn, I., McDonough, W.F., Spicuzza, M.J., Valley, J.W., Haggerty, S.E., 2002. Geochemistry of xenolithic eclogites from West Africa, part II: origins of the high MgO eclogites. *Geochim. Cosmochim. Acta*, in press.
- Beckinsale, R.D., Gale, N.H., Pankhurst, R.J., Macfarlane, A., Crow, M.J., Arthurs, J.W., Wilkinson, A.F., 1980. Discordant Rb–Sr and Pb–Pb whole rock isochron ages for the Archean basement of Sierra Leone. *Precambrian Res.* 13, 63–76.
- Black, L.P., Williams, I.S., Compston, W., 1986. Four zircon ages from one rock: the history of a 3930 Ma-old granulite from Mount Sones, Enderby Land Antarctica. *Contrib. Mineral. Petrol.* 94, 427–437.
- Boher, M., Abouchami, W., Michard, A., Albarède, F., Arndt, N.T., 1992. Crustal growth in West Africa at 2.1 Ga. *J. Geophys. Res.* 97, 345–369.
- Carlson, R.W., Pearson, D.G., Boyd, F.R., Shirey, S.B., Irvine, C., Menzies, A.H., Gurney, J.J., 1999. Re–Os systematics of lithospheric peridotites: implications for lithosphere formation and preservation. In: Gurney, J.J., Gurney, J.L., Pascoe, M.D., Richardson, S.H. (Eds.), *Proceedings of the Seventh International Kimberlite Conference*. Red Roof Design, Cape Town, pp. 99–108.
- Cocheric, A., Legendre, O., Peucat, J.J., Kouamclan, A.N., 1998. Geochronology of polygenetic monazites constrained by in situ electron microprobe Th–U-total lead determination: implications for lead behaviour in monazite. *Geochim. Cosmochim. Acta* 62, 2475–2497.
- Corfu, F., 2000. Extraction of Pb with artificially too-old ages during stepwise dissolution experiments on Archean zircon. *Lithos* 53, 279–291.
- Fung, A.T., Haggerty, S.E., 1995. Petrography and mineral compositions of eclogites from the Koidu Kimberlite complex, Sierra Leone. *J. Geophys. Res.* 100, 20451–20473.
- Graham, S., Lambert, D.D., Shee, S.R., Smith, C.B., Hamilton, R., 1999. Re–Os and Sm–Nd isotopic constraints on the sources of kimberlites and melnoites, Earahedy basin, Western Australia. In: Gurney, J.J., Gurney, J.L., Pascoe, M.D., Richardson, S.H. (Eds.), *Proceedings of the Seventh International Kimberlite Conference*. Red Roof Design, Cape Town, pp. 280–290.
- Harrison, W.J., Wood, B.J., 1980. An experimental investigation of the partitioning of REE between garnet and liquid with reference to the role of defect equilibria. *Contrib. Mineral. Petrol.* 72, 145–155.
- Hedge, C.E., Marvin, R.F., Naeser, C.W., 1975. Age provinces in the basement rocks of Liberia. *J. Res. US Geol. Surv.* 3, 425–429.
- Helmstaedt, H., Doig, R., 1975. Eclogite nodules from kimberlite pipes of the Colorado Plateau—samples of subducted Franciscan-type oceanic lithosphere. *Phys. Chem. Earth* 9, 95–111.
- Hills, D.V., Haggerty, S.E., 1989. Petrochemistry of eclogites from the Koidu Kimberlite complex, Sierra Leone. *Contrib. Mineral. Petrol.* 103, 397–422.
- Horn, I., Rudnick, R.L., McDonough, W.F., 2000. Precise elemental and isotopic ratio determination by combined

- solution nebulization and laser ablation ICP-MS: application to U/Pb geochronology. *Chem. Geol.* 164, 281–301.
- Hurley, P.M., Leo, G.W., White, R.W., Fairbairn, H.W., 1971. Liberian age province (about 2700 million year) and adjacent provinces in Liberia and Sierra Leone. *Geol. Soc. Am. Bull.* 82, 3483–3490.
- Hurley, P.M., Fairbairn, H.W., Gaudette, H.E., 1975. Progress report on early Archean Rocks in Liberia, Sierra Leone and Guayana, and their general stratigraphic setting. In: Windley, B.F. (Ed.), *The Early History of the Earth*. Wiley, London, pp. 511–521.
- Ireland, T.R., Rudnick, R.L., Spetsius, Z., 1994. Trace elements in diamond inclusions from eclogites reveal link to Archean granites. *Earth Planet. Sci. Lett.* 128, 199–213.
- Jacob, D., Jagoutz, E., Lowry, D., Matthey, D., Kudrjavitseva, G., 1994. Diamondiferous eclogites from Siberia: remnants of Archean oceanic crust. *Geochim. Cosmochim. Acta* 58, 5195–5207.
- Kouamelan, A.N., Delor, C., Peucat, J.-J., 1997. Geochronological evidence for reworking of Archean terrains during the early Proterozoic (2.1 Ga) in the western Cote d'Ivoire (man rise-West African craton). *Precambrian Res.* 86, 177–199.
- Kröner, A., Ekwueme, B., Pidgeon, R., 2001. The oldest rocks in West Africa: SHRIMP zircon age for early Archean migmatitic orthogneiss at Kaduna, northern Nigeria. *J. Geol.* 109, 399–406.
- Longerich, H.P., Jackson, S.E., Günther, D., 1996. Laser ablation inductively coupled plasma mass spectrometric transient signal data acquisition and analyte concentration calculation. *J. Anal. Atom. Spectrom.* 11, 899–904.
- Ludwig, K.R., 1998. *ISOPLOT/EX* (Special Publication 1). Berkeley Geochronological Center.
- Macfarlane, A., Crow, M.J., Arthurs, J.W., Wilkinson, A.F., Aucott, J.W., 1981. The geology and mineral resources of northern Sierra Leone. *Overseas Mem. Inst. Geol. Sci.* 7, 103.
- MacGregor, I.D., Manton, W.I., 1986. Roberts Victor eclogites: ancient oceanic crust. *J. Geophys. Res.* 91, 14063–14079.
- Martin, H., 1994. The Archean grey gneisses and the genesis of continental crust. In: Condie, K.C. (Ed.), *Archean Crustal Evolution. Developments in Precambrian Geology*. Elsevier, Amsterdam, pp. 205–259.
- Menzies, A.H., Shirey, S.B., Carlson, R.W., Gurney, J.J., 1998. Re–Os systematics of diamond-bearing eclogites and peridotites from Newlands Kimberlite. *Seventh International Kimberlite Conference*, Cape Town, pp. 579–581.
- Mezger, K., Essene, E.J., Halliday, A.N., 1992. Closure temperatures of the Sm–Nd system in metamorphic garnets. *Earth Planet. Sci. Lett.* 113, 397–409.
- Nutman, A.P., Bennett, V.C., Friend, C.R.L., McGregor, V.R., 2000. The early Archean Itsaq gneiss complex of southern West Greenland: the importance of field observations in interpreting age and isotopic constraints for early terrestrial evolution. *Geochim. Cosmochim. Acta* 64, 3035–3060.
- Pearson, D.G., Carlson, R.W., Shirey, S.B., Boyd, F.R., Nixon, P.H., 1995a. Stabilisation of Archean lithospheric mantle: a Re–Os isotope study of peridotite xenoliths from the Kaapvaal craton. *Earth Planet. Sci. Lett.* 134, 341–357.
- Pearson, D.G., Snyder, G.A., Shirley, S.B., Taylor, L.A., Carlson, R.W., Sobolev, N.V., 1995b. Archean Re–Os age for Siberian eclogites and constraints on Archean tectonics. *Nature* 374, 711–713.
- Pidgeon, R.T., Nemchin, A.A., Hitchen, G.J., 1998. Internal structures of zircons from Archean granites from the Darling range batholith: implications for zircon stability and the interpretation of zircon U–Pb ages. *Contrib. Mineral. Petrol.* 132, 288–299.
- Poldervaart, A., 1956. Zircons in rocks. 2. Igneous rocks. *Am. J. Sci.* 254, 521–544.
- Potrel, A., Peucat, J., Fanning, C.M., Auvray, B., Burg, J.P., Caruba, C., 1996. Old terranes (3.5 Ga) in the West African craton, Mauritania. *J. Geol. Soc. London* 153, 507–510.
- Potrel, A., Peucat, J.J., Fanning, C.M., 1998. Archean crustal evolution of the West African Craton; example of the Amsaga area (reguibat rise); U–Pb and Sm–Nd evidence for crustal growth and recycling. *Precambrian Res.* 90, 107–417.
- Reischmann, T., 1995. Precise U/Pb age determination with baddeleyite (ZrO₂), a case study from the Phalaborwa igneous complex, South Africa. *S. Afr. J. Geol.* 98, 1–4.
- Rollinson, H., 1997. Eclogite xenoliths in west African kimberlites as residues from Archean granitoid crust formation. *Nature* 389, 173–176.
- Rollinson, H.R., Cliff, R.A., 1982. New Rb–Sr age determinations on the Archean basement of eastern Sierra Leone. *Precambrian Res.* 17, 63–72.
- Roy-Barman, M., Allègre, C.J., 1994. ¹⁸⁷Os/¹⁸⁶Os ratios of mid-ocean ridge basalts and abyssal peridotites. *Geochim. Cosmochim. Acta* 58, 5043–5054.
- Rudnick, R.L., Williams, I.S., 1987. Dating the lower crust by ion microprobe. *Earth Planet. Sci. Lett.* 85, 145–161.
- Schulze, D.J., Valley, J.W., Viljoen, K.S., Stiefenhofer, J., Spicuzza, M., 1997. Carbon isotope composition of graphite in mantle eclogites. *J. Geol.* 105, 379–386.
- Shirey, S.B., Walker, R.J., 1995. Carius tube digestion for low-blank rhenium–osmium analysis. *Anal. Chem.* 67, 2136–2141.
- Shirey, S.B., Carlson, R.W., Richardson, S.H., Menzies, A., Gurney, J.J., Pearson, D.G., Harris, J.W., Wiechert, U., 2001. Archean emplacement of eclogite components into the lithospheric mantle during formation of the Kapvaal craton. *Geophys. Res. Lett.* 28, 2509–2512.
- Snyder, G.A., Jerde, E.A., Taylor, L.A., Halliday, A.N., Sobolev, V.N., Sobolev, N.V., 1993. Nd and Sr isotopes from diamondiferous eclogites, Udachnaya Kimberlite pipe, Yakutia, Siberia: evidence of differentiation in the early Earth. *Earth Planet. Sci. Lett.* 118, 91–100.
- Stacey, J.S., Kramers, J.D., 1975. Approximation of terrestrial lead isotope evolution by a two-stage model. *Earth Planet. Sci. Lett.* 26, 207–221.

- Taylor, L.A., Neal, C.R., 1989. Eclogites with oceanic crustal and mantle signatures from the Bellsbank kimberlite, South Africa, part I: mineralogy, petrography, and whole rock chemistry. *J. Geol.* 97, 551–567.
- Tera, F., Wasserburg, G.J., 1972. U–Th–Pb systematics in three Apollo 14 basalts and the problem of initial Pb in lunar rocks. *Earth Planet. Sci. Lett.* 14, 281–304.
- Thiéblemont, D., Delor, C., Cocherie, A., Lafon, J.M., Goujou, J.C., Baldé, A., Bah, M., Sané, H., Fanning, C.M., 2001. A 3.5 Ga granite–gneiss basement in Guinea: further evidence for early Archean accretion within the West African craton. *Precambrian Res.* 108, 179–194.
- Walker, R.J., Carlson, R.W., Shirey, S.B., Boyd, F.R., 1989. Os, Sr, Nd, and Pb isotope systematics of southern African peridotite xenoliths: implications for the chemical evolution of subcontinental mantle. *Geochim. Cosmochim. Acta* 53, 1583–1595.
- Wiedenbeck, M., Alle, P., Corfu, F., Griffin, W.L., Meier, M., Ober, F., von Quandt, A., Roddick, J.C., Spiegel, J., 1995. Three natural zircon standards for U–Th–Pb, Lu–Hf, trace element and REE analyses. *Geostand. Newslett.* 19, 1–23.
- Williams, H.R., 1978. The Archaean geology of Sierra Leone. *Precambrian Res.* 6, 251–268.